Biointerface Research in Applied Chemistry
Open-Access Journal (ISSN: 2069-5837)

Article
Volume 16, Issue 1, 2026, 24
https://doi.org/10.33263/BRIAC161.024

In Silico Evaluation of Bioactive Compounds from Sungkai Leaves (*Peronema canescens* Jack) as Potential Allosteric Activators of Catalase (CAT)

Muhammad Marsha Azzami Hasibuan [1], Dimas Andrianto [1], Raden Haryo Bimo Setiarto [2,*]

[1] Department of Biochemistry, IPB University, Bogor, 16680, Indonesia; m.marsha2001@gmail.com (M.M.A.H.); dimasandrianto@apps.ipb.ac.id (D.A.);
[2] Research Center for Applied Microbiology, National Research and Innovation Agency (BRIN), KST Soekarno, Cibinong, Bogor, 16911, Indonesia
* Correspondence: rhar002@brin.go.id (R.H.B.S.);

Received: 7.08.2025; Accepted: 28.10.2025; Published: 15.02.2026

Abstract: Reactive oxygen species (ROS) are highly reactive molecules produced during normal metabolism that can cause oxidative stress when accumulated. Catalase (CAT) is a key antioxidant enzyme that decomposes hydrogen peroxide into water and oxygen, maintaining cellular redox balance. This study investigated bioactive compounds from *Peronema canescens* (Sungkai) leaves as potential allosteric activators of catalase using an integrated in silico approach. Forty-three phytochemicals were evaluated through ADMET profiling, toxicity prediction, and molecular docking against the catalase allosteric site. Global and local reactivity descriptors, structure–activity relationships (SAR), and bioactivity radar analyses were applied to assess drug-likeness and pharmacological potential. Among the tested ligands, SMR000036195 (2-oxo-6-(piperidin-1-sulfonyl)-benzothiazole-3-carboxylic acid isobutyl ester) exhibited the strongest binding affinity (–7.63 kcal/mol), surpassing the reference activator D-trehalose (–6.07 kcal/mol). The compound also demonstrated favourable pharmacokinetic and safety profiles, suggesting low toxicity and good bioavailability. Key residue interactions indicated stable allosteric binding that may enhance catalase activity through conformational modulation. These findings propose SMR000036195 as a promising natural allosteric activator of catalase, potentially contributing to the development of antioxidant therapies targeting oxidative stress–related disorders. Further in vitro and in vivo studies are warranted to validate its enzyme activation and therapeutic potential.

Keywords: allostery; catalase; molecular docking; Sungkai; YASARA.

© 2026 by the authors. This article is an open-access article distributed under the terms and conditions of the Creative Commons Attribution (CC BY) license (https://creativecommons.org/licenses/by/4.0/), which permits unrestricted use, distribution, and reproduction in any medium, provided the original work is properly cited. The authors retain copyright of their work, and no permission is required from the authors or the publisher to reuse or distribute this article, as long as proper attribution is given to the original source.

1. Introduction

Reactive oxygen species (ROS) are reactive by-products of aerobic metabolism that play dual roles in biological systems, acting as essential signalling molecules at physiological levels but causing oxidative stress when excessively accumulated. Elevated ROS can damage lipids, proteins, and nucleic acids, contributing to chronic diseases such as cancer, neurodegenerative disorders, diabetes, and cardiovascular dysfunctions [1]. Among endogenous antioxidant defences, catalase (CAT) is one of the most efficient enzymes for detoxifying hydrogen peroxide into water and oxygen, thereby maintaining cellular redox

homeostasis. Catalase is widely distributed in living organisms and is particularly abundant in the liver, where it mitigates oxidative injury arising from metabolic processes. Its proper activity is vital for cellular protection and longevity [2,3].

Natural bioactive compounds from plants have gained increasing attention as modulators of antioxidant enzymes. Polyphenols, flavonoids, and terpenoids, commonly found in medicinal plants, have been reported to enhance catalase activity through structural stabilisation or transcriptional upregulation [3,4]. *Peronema canescens* Jack (Sungkai), a traditional Indonesian medicinal plant, is rich in these phytochemicals and exhibits broad antioxidant, anti-inflammatory, and antimicrobial properties. However, its potential as a source of natural catalase activators has not yet been explored [5,6]. Previous in silico research on catalase has primarily focused on enzyme inhibition, structure–function characterisation, or binding interactions with compounds such as curcumin or tobacco-derived metabolites [5–7]. Studies specifically addressing catalase activation through allosteric modulation by plant-derived metabolites remain scarce [8].

Therefore, this study investigates the molecular interaction between Sungkai phytoconstituents and catalase using computational approaches, including bioavailability prediction, toxicity assessment, and molecular docking. The aim is to identify Sungkai-derived compounds that function as natural allosteric activators of catalase, providing a novel framework for antioxidant enzyme modulation and future therapeutic development.

2. Materials and Methods

2.1. Materials.

This study was conducted on a computer running Windows 11 Professional 64-bit, featuring an AMD Ryzen 5 5600H processor @3.30GHz-4.20GHz and an NVIDIA RTX 3060 GPU. The software used included Yet Another Scientific Artificial Reality Application (YASARA) Structure, BIOVIA Discovery Studio 2024, and ChimeraX. All test ligands were downloaded from PubChem (https://pubchem.ncbi.nlm.nih.gov), and the receptors were downloaded from the RCSB PDB (https://www.rcsb.org).

2.2. Methods.

2.2.1. Protein functional sites.

Research on the functional sites of the identified protein was performed using CD-search on the CDD webserver11 (ncbi.nlm.nih.gov/Structure/cdd/wrpsb.cgi) at three interfaces, including the haeme-binding pocket, NADPH-binding site, and active site [8]. Allosteric functional sites were predicted using the ASD website (mdl.shsmu.edu.cn/ASD) and AllositePro Software (mdl.shsmu.edu.cn/AST/) [9,10].

2.2.2. Pharmacokinetic test.

The molecular structures of the 42 bioactive compounds from *Peronema canescens* Jack were obtained from PubChem. Pharmacokinetics is one of the most crucial pieces of information to gather before beginning research on the identification and creation of novel therapeutic therapies. Typically, this is accomplished using separate indicators known as absorption, distribution, metabolism, excretion, and toxicity (ADMET) factors. Using the online SwissADME software (swissadme.ch), various ADME parameters were computed for

this study (swissadme.ch), such as Intestinal Absorption, AMES Toxicity, and hERG blockers [11,12]. Using pkCSM (biosig.lab.uq.edu.au/pkcsm/prediction) and Deep-PK (biosig.lab.uq.edu.au/deeppk/), additional information related to ADMET properties and pharmacokinetic parameters was identified [12,13].

2.2.3. Toxicity prediction.

The toxicity of the compounds was predicted to ensure their safety in humans. The analysis was performed using ProTox-III (tox.charite.de/protox3), a virtual lab for predicting the toxicities of small molecules. The drugs were uploaded to the server, which yielded results showing the toxicity prediction in comparison to already reported drugs, such as Abacavir and Azelastine [14].

2.2.4. Ligand and receptor preparation.

The test ligands were obtained from the PubChem database. The 1DGF protein was selected as the target receptor and imported into the Yasara Structure software. The protein structure was prepared by adding a hydrogen atom, removing the water molecules, and deleting any unused ligands. The test compounds were then optimised by minimising their binding energies using the "Energy minimisation" experiment in the YASARA Structure program. Both the receptor and ligand were saved in *.pdb file format [15].

2.2.5. Molecular docking between ligands and receptor.

Docking simulations were validated to ensure the reliability and reproducibility of the predicted binding interactions. Validation was performed by redocking the native ligand into the catalase (CAT) active site to assess the accuracy of the docking protocol. The resulting root mean square deviation (RMSD) between the crystallographic and redocked poses was below 2.0 Å, confirming acceptable accuracy [15]. The docking grid box was centered on the catalase allosteric site with dimensions of 40 × 40 × 40 Å to encompass the active residues. Exhaustiveness was set to 8 to balance search thoroughness and computational efficiency. All docking simulations were conducted using AutoDock Vina, and the binding affinity (ΔG) values were reported in kcal/mol. The scoring convention follows that more negative binding energies indicate stronger predicted ligand–receptor interactions. All parameters and settings were kept consistent across all test ligands to enable comparative evaluation [16].

The receptor was docked with the ligands using YASARA. Redocking was performed to determine the most suitable grid box size. This process was continued for screening. The YASARA structure with the dock_run.mcr.macro script was executed with 100 runs, and the Amber14 force field was used for validation [16]. The dock_runscreening macro file, written by Elmar Krieger for the YASARA structure, was used to attach an unlimited number of ligands to the target receptor using the VINA or AutoDock methods. The resulting binding energy values were sorted accordingly (yasara.org/dock_runscreening.mcr). Screening was performed using the YASARA structure with the macrodock_runscreening.mcr set in the VINA method, runs=100, and Amber14 [15].

All docking experiments were performed using AutoDock Vina v1.2.3 integrated within the YASARA Structure package v22.9.26 [15,16]. Protein and ligand preparations, including hydrogen addition, charge assignment, and energy minimisation, were executed using YASARA's AutoDock-compatible workflow. Post-docking visualization, hydrogen

bond mapping, and hydrophobic surface analysis were performed using Discovery Studio Visualizer v21.1.0 [15]. Binding affinity (ΔG) values were expressed in kcal/mol, following the convention that more negative scores indicate stronger predicted ligand–receptor interactions. All computational parameters were kept consistent across ligands to ensure comparability.

2.2.6. Data analysis.

BIOVIA Discovery Studio 2024 and ChimeraX version 1.8 were used to analyse and visualise the screening data in two and three dimensions. Using the YASARA structure, the (. yob) files, or objects containing complexes, are transformed into (. pdb) format for simpler 2D and 3D visualisation using BIOVIA Discovery Studio and ChimeraX [16].

3. Results and Discussion

The test ligands used in this study were 42 active compound ligands of *Peronema canescens* Jack and one comparison ligand, D-trehalose [17]. The first physicochemical test performed was the Lipinski Rules of Five. Four ligands were eliminated from the 43 ligands tested. ADMET parameters, including intestinal absorption, AMES toxicity, hERG blockers, carcinogenesis, and LD_{50}, were used to test the remaining 39 ligands. Thirteen of the 39 ligands that were evaluated were eliminated, and the remaining ligands proceeded to the next phase of evaluation. Five compounds with the best Gibbs free energy values were selected through virtual screening of 26 test ligands. After docking the five ligands with the receptor, the results were compared with those of the docking of D-trehalose. Based on the interaction between the ligand and receptor, the best ligands were visualised and compared with D-trehalose.

3.1. Pharmacokinetic test.

The Lipinski rules of 5 (

Table **1**) pharmacokinetic criteria are important when researching drug-like compounds. The criteria of the Lipinski Rules of 5 include molecular weight, log P, rotatable bonds, donors and acceptors, and surface area. If a compound fails one or more of these rules, it can be predicted to have a bioavailability problem. Lipinski's rule describes the physicochemical properties of compounds based on predetermined criteria [13]. Of the 43 ligands tested, four were eliminated. The bioavailability radars of the top five ligands that passed the bioavailability test and D-trehalose are shown in Figure 1.

The remaining 39 ligands were tested using ADMET parameters, such as intestinal absorption, AMES toxicity, hERG Blockers, Carcinogenesis, and LD_{50}. Of the 39 ligands tested, 13 were eliminated, and the remaining ligands advanced to the next test stage. Virtual screening showed that among the 26 test ligands, five compounds showed the best Gibbs free energy values.

Table 1. Results of Lipinski's rules of the 5 bioavailability test and ADMET test.

Ligand	Lipinski's Rules of 5						ADMET				
	MW	**Intestinal absorption**	**AMES toxicity**	**hERG blockers**	**Hepatotoxicity**	**LD_{50}**	**Intestinal absorption**	**AMES toxicity**	**hERG blockers**	**Hepatotoxicity**	**LD50**
Acceptable value	≤ 500	>0.3	Safe	Safe	Safe	≥300 mg/kg	>0.3	Safe	Safe	Safe	≥300 mg/kg
DTXSID50454478	398.52	1.00	Toxic	Safe	Toxic	1000 mg/kg, Class 4	1.00	Toxic	Safe	Toxic	1000 mg/kg, Class 4

Ligand	Lipinski's Rules of 5						ADMET				
	MW	Intestinal absorption	AMES toxicity	hERG blockers	Hepatotoxicity	LD_{50}	Intestinal absorption	AMES toxicity	hERG blockers	Hepatotoxicity	LD50
SMR000036195	382.43	0.98	Safe	Safe	Safe	2730 mg/kg, Class 5	0.98	Safe	Safe	Safe	2730 mg/kg, Class 5
Prednisone	358.43	1.00	Toxic	Safe	Toxic	1680 mg/kg, Ckass 4	1.00	Toxic	Safe	Toxic	1680 mg/kg, Ckass 4
CHEMBL2440886	372.55	0.96	Safe	Safe	Safe	1000 mg/kg, Class 4	0.96	Safe	Safe	Safe	1000 mg/kg, Class 4
Glycidyl Oleate	338.52	0.75	Safe	Safe	Safe	3520 mg/kg, Class 5	0.75	Safe	Safe	Safe	3520 mg/kg, Class 5
D - Trehalose	342.30	0.04	Safe	Safe	Safe	29700 mg/kg, Class 6	0.04	Safe	Safe	Safe	29700 mg/kg, Class 6

The red ligand violates one or more of the Lipinski Ro5 test parameters.

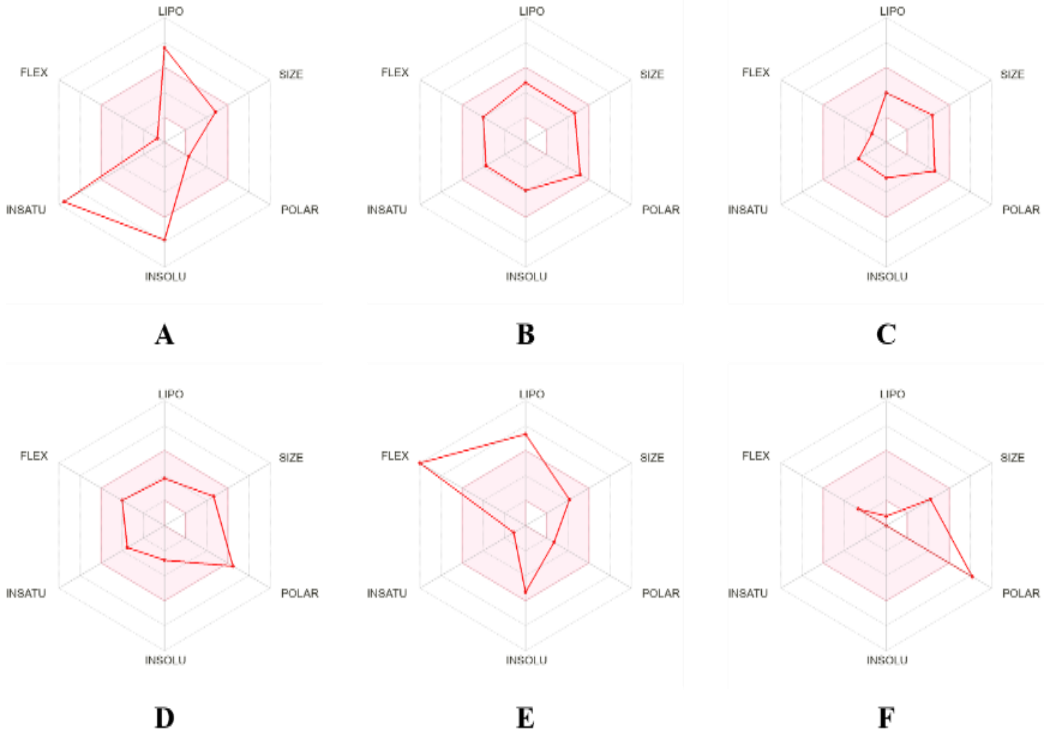

Figure 1. Bioavailability of the Catalase test ligands. **(A)** DTXSID50454478; **(B)** SMR000036195; **(C)** Prednisone; **(D)** CHEMBL2440886; **(E)** Glycidyl Oleate; **(F)** D-trehalose.

The five ligands were then docked to the receptor, and the results were compared with those from D-trehalose docking. 1 describes the results of several criteria selected from ADMET, including intestinal absorption (>30% to be in the safe category), AMES toxicity ("safe" result to enter the safe category), Human Ether-A-Go-Go Related Gene (hERG) blocker ("safe" result to enter the safe category) carcinogenesis ("Safe" result to enter the safe category), and LD_{50} (> 300 mg/KgBW/day to enter the safe category) [13,14].

Lipinski established criteria for pharmacokinetic screening, stating that the most "drug-like" molecules should have a topological polar surface area (TPSA) of ≤ 140 Å², a log P value of ≤ 5, a molecular weight of ≤ 500, and no more than 10 hydrogen bond acceptors or donors. Issues with bioavailability may arise when molecules fail to meet one or more of these requirements [18]. The rule of 5 refers to a pattern that reflects the important numbers 5, 500,

2 × 5, and 5. The fifth and sixth requirements were to have no more than 10 rotatable bonds and a maximum of 12 hydrogen bond donors and acceptors combined. Drug absorption in the human body begins in the intestinal epithelium, then moves into the circulation, and finally reaches the drug's site of action. Prior research has demonstrated that molecules weighing more than 500 Da typically have less-than-ideal absorption properties [18]. As shown in

Table 1, all the tested ligands successfully met these criteria.

The acceptable limit for lipophilicity is Log P < 5, according to the second criterion. Drug candidates that exceed this limit often exhibit lower solubility in physiological fluids, preventing them from reaching the membrane surface. Overly hydrophilic compounds may find it difficult to pass across cell membranes and reach their target sites of action, whereas excessively hydrophobic compounds (Log P > 5) tend to remain at the first membrane they come into contact with [18]. The number of hydrogen bond donors and acceptors significantly affects a molecule's physicochemical properties, including solubility, absorption, and distribution, which directly influence drug efficacy. For optimal absorption and permeability, the number of hydrogen bond donors should be less than 5, and the number of acceptors should be less than 10. If a compound does not adhere to this guideline, it may be too polar to pass through cell membranes effectively [18]. As shown in

Table 1, only D-trehalose failed to meet the hydrogen-acceptor criteria.

Rotatable bonds (Rot. Bonds) are defined as single non-ring bonds connected to a non-terminal heavy atom (i.e., a non-hydrogen atom). Amide C-N bonds are excluded from this definition because of their high rotational energy barriers. This straightforward topological parameter serves as an indicator of molecular flexibility and has been shown to be a reliable predictor of the oral bioavailability of drugs [18]. As shown in Figure 1, all test ligands passed this test. The topological polar surface area (TPSA) of drug molecules directly affects their absorption through biological membranes, such as those in $CaCO^{-2}$ cells (large intestine carcinoma) and in brain and nerve cells within the central nervous system. Drugs with a dynamic TPSA of less than 60 $Å^2$ are fully absorbed, whereas those with a TPSA greater than 140 $Å^2$ experience limited permeability [19]. Based on

Table 1, only D-trehalose failed to meet the TPSA criteria.

One of the most important criteria is the assessment of the pharmacokinetic and pharmacodynamic characteristics of drug molecules. Designing new drug candidates requires an understanding of ADMET properties. Both good ADMET properties and effective therapeutic activity are essential for successful drug development. A key component of drug development is understanding how medications are absorbed, especially when taken orally, and how the digestive system absorbs them. Neurotoxicity and nephrotoxicity can occur due to distribution and metabolism, which are negatively affected by suboptimal absorption. Therefore, this study aimed to clarify how drug molecules behave in an organism by analysing ADMET features, which are crucial for computational drug design [12,20].

A compound that enters the bloodstream can reach the tissue. Drugs are usually administered through mucous surfaces, such as the digestive tract, before the target cells absorb them. Chemical instability in the stomach, intestinal transit time, gastric emptying time, poor compound solubility, and inability to cross the intestinal wall limit drug absorption after oral administration. Poorly absorbed drugs are not well suited for oral delivery, such as intravenous or inhaled delivery [12,13]. A molecule with an Intestinal Absorption of less than 30% is considered poorly absorbed. As shown, D-trehalose failed this test.

AMES toxicity testing is a commonly used method for evaluating the mutagenic potential of drugs using bacterial assays. A positive result from this test suggests that the compound being studied may be mutagenic and could potentially act as a carcinogen. [13,14,21]. Based on Pires et al. [13], DTXSID50454478 and prednisone failed the test. The criteria for hERG inhibitors indicate that the blockage of potassium channels encoded by the hERG (human ether-a-go-go gene) is a key factor in the development of QT syndrome, which can lead to serious ventricular arrhythmias [13]. All test ligands passed this test. Drug-induced liver injury (DILI) is a significant safety issue in drug development and a major reason for the failure of drugs in the market. A compound is classified as hepatotoxic if it is linked to at least one pathological or physiological liver event that is closely associated with impaired liver function. DTXSID50454478 and prednisone failed the test.

The potential toxicity of compounds is important. The lethal dosage value (LD_{50}) is a standard measure of acute toxicity used to assess toxicity relative to other molecules. LD_{50} is the amount of compound administered directly capable of causing the death of 50% of the test animals. In ProTox-III, there are six, which are fatal. On the other hand, class 6 shows classes for toxicity (1 to 6), in which class 1 has $LD_{50} \leq 5$, which is fatal if consumed up to $LD_{50} > 5000$, which means the compound is non-toxic [14]. All test ligands passed this test.

3.2. Molecular docking between ligands and receptor.

The Grid box size used for the screening was 2 Å because it yielded an RMSD of 0 Å and a binding energy of 6.07 kcal/mol during redocking. This study provides screening results on binding energy, residual contact, and the types of interactions formed. Table explains the ranking of the top five ligands based on their binding energies. A positive score indicates the best binding energy in the YASARA structure. Thus, a score with a more positive result indicates better ligand binding to the receptor [16,21]. Receptor interactions with D-trehalose are shown in Figure 2, and receptor interactions with SMR000036195 are shown in Figure 3.

Table 2. Sungkai molecular docking results in CAT.

Ligand	Effi [kcal/(mol*Atom)]	Bind.energy [kcal/mol]	Dissoc. constant[pM]
DTXSID50454478	0.34	10.15	3.61E+04
SMR000036195	0.29	7.63	2.57E+06
Prednisone	0.27	7.04	6.95E+06
CHEMBL2440886	0.28	6.91	8.61E+06
Glycidyl Oleate	0.28	6.78	1.08E+07
D - Trehalose	0.25	6.07	3.57E+07

The red ligand violates one or more pharmacokinetic test parameters.

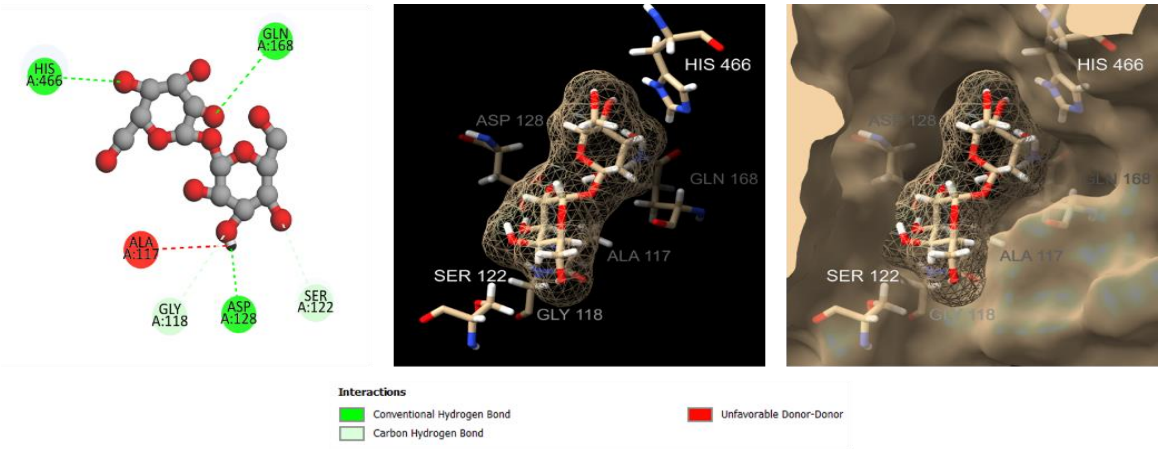

Figure 2. D-trehalose interaction with catalase receptor visualized in 2D and 3D.

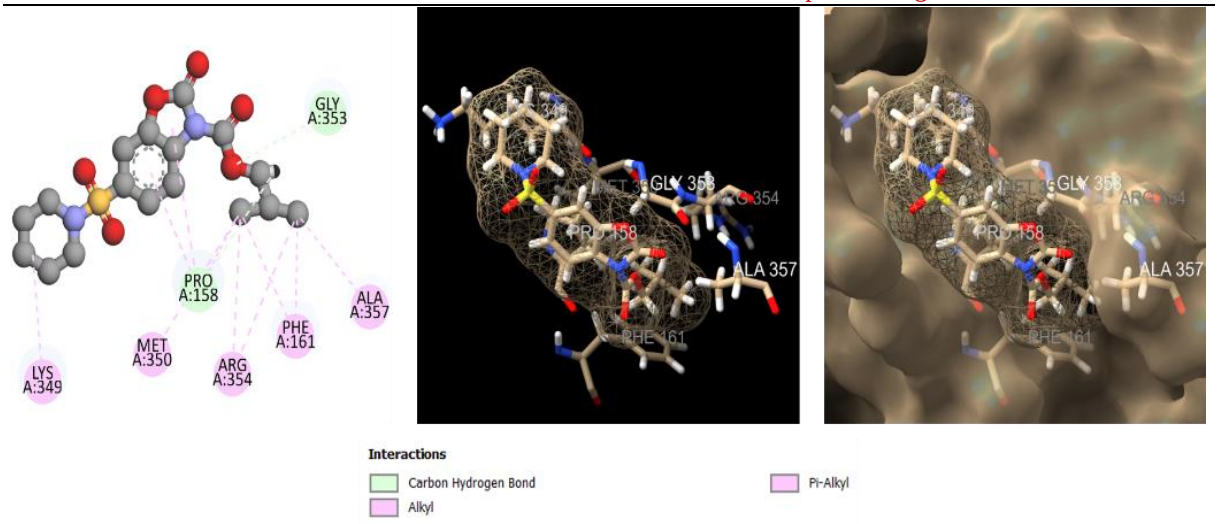

Figure 3. SMR000036195 interaction with catalase receptor visualized in 2D and 3D.

The table shows the interactions between each test ligand, divided into two categories: hydrogen and hydrophobic bonds. The more hydrogen bonds a ligand forms, the easier and stronger the ligand binds to the active site of the receptor. In contrast, hydrophobic bonds are considered important because of their role in stabilising the interaction between ligands and receptors [22]. Molecular docking was performed to examine interactions between the receptor and the ligand. The test ligands and receptors used were identified through screening in a previous test. In this study, molecular docking was performed using a targeted docking approach on allosteric sites.

In addition, a small Kd value indicates stronger ligand binding to the receptor [16,23]. The ligand efficiency of SMR000036195 was 0.29, whereas that of D-trehalose was 0.25, indicating that the binding energy contributed per atom of the compounds was similar to the required energy to develop key contacts with the catalase target [16,24]. The ligand efficiency range near D-trehalose (based on the binding energy) was 0.28–0.34. Based on Lipinski Ro5, ADMET, and molecular docking with the catalase receptor, we selected SMR000036195 as the best test ligand for consideration as an alternative allosteric activator.

Table 3. Residue interaction analysis between test ligands and CAT.

Ligand	Residues/Amino acids involved	
	Hydrophobic Interaction	**Hydrogen Bond**
D-trehalose		A GLY 118, A SER 122, A ASP 128, A GLN 168, A HIS 466
DTXSID50454478	A VAL 73, A VAL 74, A ILE 159, A PHE 161, A PRO 162, A ALA 357	
SMR000036195	A PRO 158, A PHE 161, A LYS 349, A MET 350, A ARG 354, A ALA 357	A PRO 158, A GLY 353
Prednisone	A TYR 325, A PHE 326	A ARG 68, A LYS 77, A SER 120,
CHEMBL2440886	A LEU 371, A PRO 378, A VAL 383	A ASN 142, A MET 339, A GLY 420
Glycidyl Oleate	A ARG 72, A VAL 73, A VAL 74, A ALA 133, A VAL 146, A PHE 161, A ALA 357, A TYR 358, A HIS 362	

Amino acids in bold indicate the presence of contact with the predicted allosteric sites.

The prediction from the conserved domain database (CDD) server revealed conservation of the active-site residues HIS 75 and ASN 148. The NADP+ binding sites were HIS 194, SER 201, ARG 203, ASP 213, LYS 237, TRP 303, HIS 305, and LYS 306. The haeme-binding site is TYR 358 [25]. The prediction result for allosteric site residue were PRO 70, GLU 71, ARG 72, VAL 73, VAL 74, HIS 75, ARG 112, SER 114, VAL 116, ALA 117,

ASP 128, PRO 129, GLY 131, PHE 132, ALA 133, VAL 146, GLY 147, ASN 148, ILE 152, PHE 153, PHE154, PRO 158, ILE 159, PHE 161, PRO 162, PHE 164, ILE 165, GLN 168, LYS 169, LEU 199, GLY 216, SER 217, HIS 218, LEU 299, ILE 332, ALA 333, PHE 334, MET 350, GLY 353, ARG 354, PHE 356, ALA 357, TYR 358, THR 361, HIS 362, HIS 364, ARG 365 [9,10,26].

D-trehalose was used as a binding energy control, so that the test ligand with a binding energy above that of D-trehalose could be considered a potential ligand for development. Based on Table , the ligand used as a control, D-trehalose (CID_7427), had a binding energy of 5.09 kcal/mol. The test ligands with binding energies above that of D-trehalose are DTXSID50454478 (10.15 kcal/mol), SMR000036195 (7.63 kcal/mol), Prednisone (7.03 kcal/mol), CHEMBL2440886 (6.91 kcal/mol), and Glycidyl Oleate (6.78 kcal/mol). The YASARA structure identified the best-scoring receptor–ligand complex. Therefore, a score with a more positive result indicates better ligand binding to the receptor [16].

In addition, a small Kd value indicates stronger ligand binding to the receptor [16,23]. The ligand efficiency of SMR000036195 was 0.29, whereas that of D-trehalose was 0.25, indicating that the binding energy contributed per atom of the compounds was similar to the required energy to develop key contacts with the catalase target [16,24]. The range of ligand efficiency of D-trehalose (based on the binding energy) was 0.28–0.34. Based on Lipinski Ro5, ADMET, and molecular docking with the catalase receptor, we selected SMR000036195 as the best test ligand for consideration as an alternative allosteric activator.

D-trehalose (Figure 2) was the ligand used as the allosteric activator standard in this study [17,27]. D-trehalose forms two types of hydrogen bonds: conventional hydrogen bonds and carbon-hydrogen bonds. Conventional hydrogen bonds were formed at the amino acid residues ASP 128, GLN 168, and HIS 466, with the interaction distance varying from 1.81 to 2.94 Å. Carbon-hydrogen bonds were formed at the amino acid residues Gly 118 and SER 122, with interaction distances of 2.77 and 3.01 Å, respectively. SMR000036195 (Figure 3) formed both hydrogen bonds and hydrophobic interactions with the target protein. The hydrogen bond formed was a carbon-hydrogen bond that occurred at amino acid residues PRO 158 and Gly 353 with interaction distances of 2.98 and 3.01 Å, respectively. Hydrophobic bonds that occurred were divided into two kinds: alkyl and pi-alkyl bonds. Alkyl bonds were formed at amino acid residues PRO 158, LYS 349, MET 350, GLY 353, ARG 354, and ALA 357, with interaction distances ranging from 3.36 to 4.94 Å. The π-alkyl bonds were formed between amino acid residues PRO 158 and PHE 161, with the interaction distance varying from 3.85 to 5.00 Å.

Molecular docking was performed to predict interactions between the phytoconstituents of *Peronema canescens Jack* (Sungkai) and the catalase (CAT) enzyme, and to identify potential allosteric activators. Among the screened compounds, ligand SMR000036195 exhibited the strongest binding affinity, with a docking score of –7.63 kcal/mol, surpassing the reference activator D-trehalose (–6.07 kcal/mol) (Table 2). Other Sungkai metabolites demonstrated moderate binding energies ranging from –6.10 to –7.21 kcal/mol, indicating variable but favourable affinities toward the CAT binding site. The more negative binding energy of SMR000036195 indicates a stronger, potentially more stable ligand–enzyme interaction, suggesting a higher likelihood of effective allosteric modulation. Visualisation of the binding pose revealed key hydrogen bonds and hydrophobic contacts involving residues His75, Tyr358, and Asn148, which are known to contribute to catalytic stabilisation (Table 3). The comparative energy profile indicates that SMR000036195 may act as a natural allosteric

activator of catalase, making it a promising candidate for further in silico and in vitro validation [27].

Table shows the interactions between each test ligand, divided into two main categories: hydrogen and hydrophobic bonds. The more hydrogen bonds the ligand forms, hypothetically, the easier and stronger the ligand binds to the active side of the receptor. A good hydrogen bond has a distance of less than 2.3 Å. Hydrophobic bonds are important because they stabilise the interaction between ligands and receptors [22,28]. Based on Wodak et al. [28], nearly all of the formed interaction bonds occurred at the allosteric site. Allostery describes a phenomenon in which ligand binding at one region of a macromolecule alters the properties or activity of a separate functional site, allowing the molecule's behaviour to be finely regulated. This mode of regulation is central to numerous cellular processes, such as signal transduction, molecular machine function, transcriptional control, and metabolic pathways [28].

The docking analysis revealed that SMR000036195 exhibited the strongest binding affinity (–7.63 kcal/mol) toward catalase, surpassing the reference compound D-trehalose (–6.07 kcal/mol). The predicted binding conformation positioned SMR000036195 within the catalase allosteric pocket, engaging in key hydrogen bonds with His75, Tyr358, and Asn148. These residues are critical for maintaining the enzyme's active-site geometry and facilitating the conversion of hydrogen peroxide into water and oxygen. The interaction with His75, in particular, may influence the positioning of the heme group, thereby enhancing the enzyme's redox turnover efficiency. From a mechanistic perspective, the ligand's ability to stabilise peripheral residues and form hydrophobic contacts along the catalytic channel suggests a possible allosteric activation mechanism [21-23]. This may enhance substrate accessibility or promote favourable conformational dynamics necessary for catalase activity. Previous studies have shown that natural polyphenols and sugar derivatives can act as structural stabilisers or activators of antioxidant enzymes through similar mechanisms [24–26]. Consistent with these findings, the strong, stable interactions observed for SMR000036195 suggest its potential to reinforce catalase's structural integrity and functional performance under oxidative stress conditions. These results highlight the mechanistic plausibility of Sungkai-derived phytoconstituents as allosteric modulators of catalase. Further molecular dynamics simulations and experimental validation are required to confirm whether such ligand-induced conformational stabilisation translates into measurable increases in catalase activity in vitro and in vivo [27].

Allostery arises from the intrinsic physical properties of macromolecules and, potentially, other complex materials. These allosteric responses are further shaped by the cellular environment, varying under physiological and pathological conditions. An allosteric activator is a compound that binds to a regulatory site distinct from the active site and enhances an enzyme's activity. Given that most interacting residues are located within the predicted allosteric region, our findings suggest that SMR000036195 could serve as an alternative allosteric activator of CAT, functioning in place of D-trehalose, the native activator.

4. Conclusions

The evaluation of bioavailability and toxicity of *Peronema canescens* Jack (sungkai) compounds, combined with molecular docking analysis against catalase, identified SMR000036195 as a safe ligand with a stronger binding affinity than D-trehalose (–7.63 kcal/mol vs. –6.07 kcal/mol). These findings indicate that SMR000036195 may serve as a promising natural allosteric activator of catalase. However, this study is limited by its reliance

on static molecular docking data without molecular dynamics (MD) validation or experimental verification. The conformational flexibility of the enzyme–ligand complex and solvent effects were not fully explored, which may influence the predicted binding interactions. Future work should include molecular dynamics simulations to confirm complex stability, in vitro catalase activation assays to verify functional modulation, and in vivo assessments to evaluate pharmacological safety and efficacy. Additionally, structural optimisation or analog design of SMR000036195 could enhance its potency and bioavailability for potential therapeutic applications.

Author Contributions

Conceptualisation, M.M.A.H., D.A., and R.H.B.S.; methodology, D.A. and R.H.B.S.; data curation/investigation, M.M.A.H.; formal analysis, M.M.A.H., D.A., and R.H.B.S.; writing—original draft preparation, M.M.A.H., D.A., and R.H.B.S.; writing—review and editing, M.M.A.H., D.A., and R.H.B.S.; All authors contributed equally to this work and have read and agreed to the published version of the manuscript.

Institutional Review Board Statement

Not applicable.

Informed Consent Statement

Not applicable.

Data Availability Statement

Data supporting the findings of this study are available upon reasonable request from the corresponding author.

Funding

This research received no external funding.

Acknowledgments

The author would like to thank all parties who have contributed to the completion of this research. All authors made equal contributions as the main contributors to this manuscript. No funding resources were reported for this publication.

Conflicts of Interest

The authors declare no conflict of interest.

Role of Funders

The funders had no role in the design of the study, the collection, analysis, or interpretation of data, the writing of the manuscript, or the decision to publish the results.

Abbreviations

The following abbreviations are used in this manuscript:

Abbreviation	Definition
ROS	Reactive Oxygen Species
ADMET	Absorption, Distribution, Metabolism, Excretion, and Toxicity
SAR	Structure Activity Relationship
YASARA	Yet Another Scientific Artificial Reality Application
LD_{50}	Lethal Dose 50
DNA	Deoxyribonucleic Acid
TPSA	Topological Polar Surface Area
CAT	Catalase

References

1. Pizzino, G.; Irrera, N.; Cucinotta, M.; Pallio, G.; Mannino, F.; Arcoraci, V.; Squadrito, F.; Altavilla, D.; Bitto, A. Oxidative stress: Harms and benefits for human health. *Oxid. Med. Cell. Longev.* **2017**, *2017*, 8416763, https://doi.org/10.1155/2017/8416763.
2. Glorieux, C.; Calderon, P.B. Catalase, a remarkable enzyme: Targeting the oldest antioxidant enzyme to find a new cancer treatment approach. *Biol. Chem.* **2017**, *398*, 1095–1108, https://doi.org/10.1515/hsz-2017-0131.
3. Li, Y.; Li, S.; Lin, S.J.; Zhang, J.J.; Zhao, C.N.; Li, H.B. Microwave-assisted extraction of natural antioxidants from the exotic Gordonia axillaris fruit: Optimization and identification of phenolic compounds. *Molecules* **2017**, *22*, 1481, https://doi.org/10.3390/molecules22091481.
4. Kasote, D.M.; Katyare, S.S.; Hegde, M.V.; Bae, H. Significance of antioxidant potential of plants and its relevance to therapeutic applications. *Int. J. Biol. Sci.* **2015**, *11*, 982–991, https://doi.org/10.7150/ijbs.12096.
5. Nene, T.; Yadav, M.; Yadav, H.S. Plant catalase in silico characterization and phylogenetic analysis with structural modeling. *J. Genet. Eng. Biotechnol.* **2022**, *20*, 128, https://doi.org/10.1186/s43141-022-00404-6.
6. Sönmez, G.D. In silico analysis on catalase protein from Nicotiana tabaccum L. *Balikesir Univ. Fen Bilim. Enst. Derg.* **2022**, *24*, 818–829, https://doi.org/10.25092/baunfbed.1114706.
7. Najjar, F.M.; Ghadari, R.; Yousefi, R.; Safari, N.; Sheikhhasani, V.; Sheibani, N.; Moosavi-Movahedi, A.A. Studies to reveal the nature of interactions between catalase and curcumin using computational methods and optical techniques. *Int. J. Biol. Macromol.* **2017**, *95*, 550–556, https://doi.org/10.1016/j.ijbiomac.2016.11.050.
8. Marchler-Bauer, A.; Bo, Y.; Han, L.; He, J.; Lanczycki, C.J.; Lu, S.; Chitsaz, F.; Derbyshire, M.K.; Geer, R.C.; Gonzales, N.R.; Gwadz, M.; Hurwitz, D.I.; Lu, F.; Marchler, G.H.; Song, J.S.; Thanki, N.; Wang, Z.; Yamashita, R.A.; Zhang, D.; Zheng, C.; Geer, L.Y.; Bryant, S.H. CDD/SPARCLE: Functional classification of proteins via subfamily domain architectures. *Nucleic Acids Res.* **2017**, *45*, D200–D203, https://doi.org/10.1093/nar/gkw1129.
9. Huang, W.; Lu, S.; Huang, Z.; Liu, X.; Mou, L.; Luo, Y.; Zhao, Y.; Liu, Y.; Chen, Z.; Hou, T.; Zhang, J. Allosite: A method for predicting allosteric sites. *Bioinformatics* **2013**, *29*, 2357–2359, https://doi.org/10.1093/bioinformatics/btt399.
10. Song, K.; Liu, X.; Huang, W.; Lu, S.; Shen, Q.; Zhang, L.; Zhang, J. Improved method for the identification and validation of allosteric sites. *J. Chem. Inf. Model.* **2017**, *57*, 2358–2363, https://doi.org/10.1021/acs.jcim.7b00014.
11. Daina, A.; Michielin, O.; Zoete, V. SwissADME: A free web tool to evaluate pharmacokinetics, drug-likeness and medicinal chemistry friendliness of small molecules. *Sci. Rep.* **2017**, *7*, 42717, https://doi.org/10.1038/srep42717.
12. Flores-Holguín, N.; Frau, J.; Glossman-Mitnik, D. In silico pharmacokinetics, ADMET Study and conceptual DFT analysis of two plant cyclopeptides isolated from rosaceae as a computational peptidology approach. *Front. Chem.* **2021**, *9*, 708364, https://doi.org/10.3389/fchem.2021.708364.
13. Pires, D.E.V.; Blundell, T.L.; Ascher, D.B. pkCSM: Predicting small-molecule pharmacokinetic and toxicity properties using graph-based signatures. *J. Med. Chem.* **2015**, *58*, 4066–4072, https://doi.org/10.1021/acs.jmedchem.5b00104.
14. Banerjee, P.; Kemmler, E.; Dunkel, M.; Preissner, R. ProTox 3.0: A webserver for the prediction of toxicity

of chemicals. *Nucleic Acids Res.* **2024**, *52*, W513–W520, https://doi.org/10.1093/nar/gkae303.
15. Gholam, G.M.; Mahendra, F.R.; Irsal, R.A.P.; Dwicesaria, M.A.; Ariefin, M.; Kristiadi, M.; Rizki, A.F.M.; Azmi, W.A.; Artika, I.M.; Siregar, J.E. Computational exploration of compounds in Xylocarpus granatum as a potential inhibitor of Plasmodium berghei using docking, molecular dynamics, and DFT studies. *Biochem. Biophys. Res. Commun.* **2024**, *733*, 150684, https://doi.org/10.1016/j.bbrc.2024.150684.
16. Irsal, R.A.P.; Gholam, G.M.; Dwicesaria, M.A.; Chairunisa, F. Computational investigation of Y. aloifolia variegate as anti-Human Immunodeficiency Virus (HIV) targeting HIV-1 protease: A multiscale in-silico exploration. *Pharmacol. Res. Mod. Chin. Med.* **2024**, *11*, 100451, https://doi.org/10.1016/j.prmcm.2024.100451.
17. Ma, X.; Deng, D. Inhibitors and Activators of SOD, GSH-Px, and CAT. In Enzyme Inhibitors and Activators, Şentürk, M., Ed.; IntechOpen: London, **2017**.
18. Sahu, V.K.; Singh, R.K.; Singh, P.P. Extended rule of five and prediction of biological activity of peptidic HIV-1-PR inhibitors. *Future J. Pharm. Sci.* **2021**, *7*, 192, https://doi.org/10.31586/ujpp.2022.403.
19. Karami, T.K.; Hailu, S.; Feng, S.; Graham, R.; Gukasyan, H.J. Eyes on Lipinski's rule of five: A new "rule of thumb" for physicochemical design space of ophthalmic drugs. *J. Ocul. Pharmacol. Ther.* **2022**, *38*, 43–55, https://doi.org/10.1089/jop.2021.0069.
20. Chandrasekaran, B.; Abed, S.N.; Al-Attraqchi, O.; Kuche, K.; Tekade, R.K. Chapter 21 - Computer-Aided Prediction of Pharmacokinetic (ADMET) Properties. In Dosage Form Design Parameters, Tekade, R.K., Ed.; Academic Press: **2018**; Volume 2, pp. 731-755, https://doi.org/10.1016/B978-0-12-814421-3.00021-X.
21. Banerjee, P.; Dehnbostel, F.O.; Preissner, R. Prediction is a balancing act: Importance of sampling methods to balance sensitivity and specificity of predictive models based on imbalanced chemical data sets. *Front. Chem.* **2018**, *6*, 362, https://doi.org/10.3389/fchem.2018.00362.
22. Irsal, R.A.P.; Hami Seno, D.S.; Safithri, M.; Kurniasih, R. Penapisan virtual senyawa aktif sirih merah (Piper crocatum) sebagai inhibitor angiotensin converting enzyme. *J. Farmamedika (Pharmamedica J.)* **2022**, *7*, 104–113, https://doi.org/10.47219/ath.v7i2.157.
23. Aamir, M.; Singh, V.K.; Dubey, M.K.; Meena, M.; Kashyap, S.P.; Katari, S.K.; Upadhyay, R.S.; Umamaheswari, A.; Singh, S. In silico prediction, characterization, molecular docking, and dynamic studies on fungal SDRs as novel targets for searching potential fungicides against fusarium wilt in tomato. *Front. Pharmacol.* **2018**, *9*, 1038, https://doi.org/10.3389/fphar.2018.01038.
24. Patel, C.N.; Goswami, D.; Jaiswal, D.G.; Parmar, R.M.; Solanki, H.A.; Pandya, H.A. Pinpointing the potential hits for hindering interaction of SARS-CoV-2 S-protein with ACE2 from the pool of antiviral phytochemicals utilizing molecular docking and molecular dynamics (MD) simulations. *J. Mol. Graph. Model.* **2021**, *105*, 107874, https://doi.org/10.1016/j.jmgm.2021.107874.
25. Putnam, C.D.; Arvai, A.S.; Bourne, Y.; Tainer, J.A. Active and inhibited human catalase structures: Ligand and NADPH binding and catalytic mechanism. *J. Mol. Biol.* **2000**, *296*, 295–309, https://doi.org/10.1006/jmbi.1999.3458.
26. Liu, X.; Lu, S.; Song, K.; Shen, Q.; Ni, D.; Li, Q.; He, X.; Zhang, H.; Wang, Q.; Chen, Y.; Li, X.; Wu, J.; Sheng, C.; Chen, G.; Liu, Y.; Lu, X.; Zhang, J. Unraveling allosteric landscapes of allosterome with ASD. *Nucleic Acids Res.* **2020**, *48*, D394–D401, https://doi.org/10.1093/nar/gkz958.
27. Uzzaman, M.; Hasan, M.K.; Mahmud, S.; Yousuf, A.; Islam, S.; Uddin, M.N.; Barua, A. Physicochemical, spectral, molecular docking and ADMET studies of Bisphenol analogues: A computational approach. *Inform. Med. Unlocked* **2021**, *25*, 100706, https://doi.org/10.1016/j.imu.2021.100706.
28. Wodak, S.J.; Paci, E.; Dokholyan, N.V.; Berezovsky, I.N.; Horovitz, A.; Li, J.; Hilser, V.J.; Bahar, I.; Karanicolas, J.; Stock, G.; Hamm, P.; Stote, R.H.; Eberhardt, J.; Chebaro, Y.; Dejaegere, A.; Cecchini, M.; Changeux, J.P.; Bolhuis, P.G.; Vreede, J.; Faccioli, P.; Orioli, S.; Ravasio, R.; Yan, L.; Brito, C.; Wyart, M.; Gkeka, P.; Rivalta, I.; Palermo, G.; McCammon, J.A.; Panecka-Hofman, J.; Wade, R.C.; Di Pizio, A.; Niv, M.Y.; Nussinov, R.; Tsai, C.J.; Jang, H.; Padhorny, D.; Kozakov, D.; McLeish, T. Allostery in its many disguises: From theory to applications. *Structure* **2019**, *27*, 566–578, https://doi.org/10.1016/j.str.2019.01.003.

Publisher's Note & Disclaimer

The statements, opinions, and data presented in this publication are solely those of the individual author(s) and contributor(s) and do not necessarily reflect the views of the publisher and/or the editor(s). The publisher and/or the editor(s) disclaim any responsibility for the accuracy, completeness, or reliability of the content. Neither the

publisher nor the editor(s) assume any legal liability for any errors, omissions, or consequences arising from the use of the information presented in this publication. Furthermore, the publisher and/or the editor(s) disclaim any liability for any injury, damage, or loss to persons or property that may result from the use of any ideas, methods, instructions, or products mentioned in the content. Readers are encouraged to independently verify any information before relying on it, and the publisher assumes no responsibility for any consequences arising from the use of materials contained in this publication.